Computational modelling of impact tests on steel fibre reinforced concrete beams

L.J. SLUYS and R. DE BORST
Delft University of Technology, Department of Civil Engineering /
TNO Building and Construction Research

Abstract

Concrete fracture under impact loading is modelled using rate-independent and rate-dependent smeared crack representations. Both models have been used to simulate the behaviour of concrete beams with both conventional and steel-fibre reinforcement. The rate-dependent crack model turns out to be superior in the sense that it properly captures the experimentally observed distributed crack pattern, but the differences in the prediction of the global structural response are hardly noticeable.

Keywords: Composite structures, impact failure, rate-dependent fracture.

1. Introduction

The numerical simulation of the deformational behaviour of concrete beams reinforced both by conventional reinforcement and steel fibres is a complicated issue, especially if truly dynamic loading conditions are considered. Indeed, the diffuse crack pattern that develops is hard to capture accurately if smeared crack representations are used. In this contribution we shall demonstrate that it is imperative to utilise a rate-dependent crack model in order to arrive at physically realistic results. The advantages of employing a rate-dependent smeared crack model rather than a rate-independent smeared crack model are two-fold. Firstly, at high strain rates as occur during impact loading the increased tensile strength is readily contained in a rate-dependent material description (Zielinski 1982, Körmeling 1986). Secondly, a rate-dependent formulation locally preserves hyperbolicity of the field equations, a feature that is not exhibited by rate-independent models. In finite element simulations of steel-fibre reinforced concrete structures this distinction has the consequence that in the rate-dependent formulation the distributed crack pattern is predicted correctly, while highly localised, physically unrealistic crack distributions are computed in the rate-independent case. In the latter case, moreover, the computed crack pattern and strain distributions in concrete and reinforcement are fully dependent on the discretisation, which is unacceptable for predictive purposes.

In this contribution we shall focus on the numerical simulation of concrete beams that are reinforced both by steel fibres and conventional steel bars. The bars have been tested experimentally at the Institut für Massivbau und Baustofftechnologie of the University of Karlsruhe. The paper will begin with a description of the experimental set-up. Then, the geometrical modelling of the beams and material modelling of the concrete, the reinforcement and the

interface between steel and concrete will be discussed. Finally, the numerical results will be presented both for he rate-dependent and the rate-independent smeared crack representations and a comparison with the experimental data will be made.

2. Description of the test

The impact tests on the steel fibre reinforced concrete beams have been carried out at the Institut für Massivbau und Baustofftechnologie of Karlsruhe University. The aim of the research was to determine the influence of the addition of fibres to the reinforced concrete under impact loading conditions. For this reason three tests have been carried out on normal reinforced concrete beams, steel fibre reinforced concrete beams with smooth fibres (WIREX) and steel fibre reinforced concrete beams with rugged fibres (DRAMIX). The type and the amount of fibres has been varied in the programme. The test with the WIREX steel fibre mixture is used here for a comparison with a computational analysis.

The experimental set-up is shown in Figure 1. The beams have been reinforced with upper and lower steel bars. Shear reinforcement is present over the length of the beam. The amount of fibres is 1.2% of the cross-sectional area. The measurement locations are given in Figure 1. For a full description of the experimental programme the reader is referred to Eibl and Lohrmann (1993).

The loading is applied via two load cells in the centre of the beam. The time-load diagrams are given in Figure 2 and show the block-type characteristic of the loading.

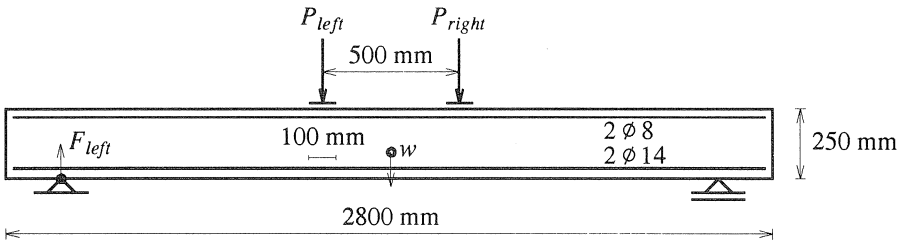

measurement locations : w - displacement centre beam
F_{left} - vertical force left support

Figure 1. Experimental set-up for impact beam test (Eibl and Lohrmann 1993).

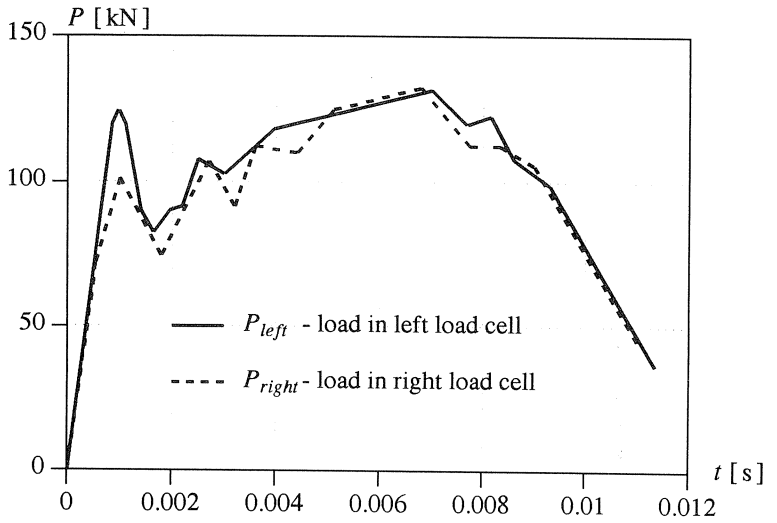

Figure 2. Time-load diagram for left and right load cell (Eibl and Lohrmann 1993).

3. Computational Modelling

The modelling of the test by means of finite elements will be discussed with successive emphasis on the geometry of the beam, the constitutive behaviour of the composite material and the deficiencies in the discretisation process.

3.1. Geometry

The beam analysis has been carried out with eight-noded plane-stress elements with a nine-point Gaussian integration. Two meshes have been used with 28 × 5 and 56 × 8 elements, respectively, for the concrete with distributed fibres. The steel reinforcement bars have been modelled with three-noded truss elements with six-noded interface elements for the modelling of bond-slip behaviour between the concrete and the reinforcement. The supports have been modelled as bilinear springs, firstly, to allow the beam to displace freely in the positive vertical direction, which occurs in an initial stadium of the test, and, secondly, to model the stiffness of the supports, which turned out to be not infinite and significantly influences the reponse.

There are two reasons for not making use of symmetry considerations. Firstly, the beam is only fixed horizontally at the left support and, therefore, the bending wave reflects in a different manner at the supports, which contributes to an asymmetry in the response. Furthermore, the load is slightly asymmetric (see Figure 2). These two effects can act as a small perturbation which can enforce an asymmetric failure mode.

3.2. Material

The composite material consists of concrete, fibres and steel bars, for which the distinct constitutive relations will be derived in this section. For the interaction between the concrete and the fibres we assume a perfect bond relation. However, the interactive forces between the concrete and the steel bars are determined via a bond-slip relation, which is the constitutive equation of the interface elements. The material data set is summarised in Table 1.

Concrete, the rate-independent and the rate-dependent concept

A rate-dependent crack model in which the stress not only depends on the crack strain but also on the crack strain rate is chosen according to

$$\sigma = f(\varepsilon_{cr}) + m \frac{\partial \varepsilon_{cr}}{\partial t} \tag{1}$$

where σ and ε_{cr} denote stress and crack strain respectively, $f(\varepsilon_{cr})$ is a softening function and m is the viscosity or material rate-sensitivity parameter. Strain decomposition of the total strain ε is applied, splitting it into an elastic strain ε_e and a crack strain ε_{cr}. Note that rate dependence is chosen to be a function of the inelastic strain ε_{cr} and not of the total strain. When a linear softening model is utilised as in this study

$$f(\varepsilon_{cr}) = f_{ct} + h\varepsilon_{cr} \tag{2}$$

eq.(1) becomes

$$\sigma = f_{ct} + h\varepsilon_{cr} + m \frac{\partial \varepsilon_{cr}}{\partial t} \tag{3}$$

In eqs.(2) and (3) f_{ct} is the initial tensile strength under static loading conditions and h is a constant softening modulus. For unloading a secant modulus without rate dependence is used. This model complies with the experimental findings that the tensile strength increases under dynamic loading (Zielinski 1982, Körmeling 1986). The complete finite element implementation is described in Sluys (1992) for the rate-dependent case, following earlier work by de Borst and Nauta (1985) and Rots (1988) on rate-independent smeared crack modelling.

In the numerical analyses in section 4 not only the rate-dependent model, but also the rate-independent model is considered. In this case two modifications have been made. Firstly the viscosity parameter $m = 0$ Ns/mm^2 and, secondly, for the tensile strength in eq.(2) the initial tensile strength under dynamic loading conditions should be filled in.

Steel reinforcement

The steel bars behave in an elasto-plastic manner with a slight hardening contribution after onset of yielding. The yield stress and the Young's modulus have been taken from dynamic tests, which have been carried out at Karlsruhe University prior to the beam tests. The values have been determined for a strain rate $\dot{\varepsilon} = 0.038$ 1/s, which is representative for the experiment.

Experimental data for the normal bond component are hardly available and cannot be transformed into a constitutive law (Rots 1988). Therefore, the interface normal behaviour and the shear normal coupling are not incorporated and the constitutive equation for the interface element reduces to a shear traction - slip relation. This slip between reinforcement and the concrete has been modelled using the relation of Dörr (Dörr 1980).

Fibre reinforcement

The fibres have been modelled according to a macroscopic approach. We do not incorporate the anisotropy in our material model as is done at a meso-level, nor do we take the distinct fibres into account as is done at a micro-level. For this larger scale engineering practice problem the macroscopic or phenomenological approach followed here is well suited to describe the constitutive behaviour of the fibre concrete. The addition of the fibres to the concrete is seen as an increase of the ductility of the cracked material and therefore the ultimate crack strain ε_{cru} is given a larger value.

concrete			
$E_{c,dyn}$	32940	[N/mm^2]	Young's modulus
ν	0.2	[-]	Poisson's ratio
$f_{ct,stat}$	3.15	[N/mm^2]	static tensile strength
$f_{ct,dyn}$	4.41	[N/mm^2]	dynamic tensile strength
ρ	2320	[kg/m^3]	density
m	2.0	[Ns/mm^2]	material rate-sensitivity parameter
steel reinforcement			
$E_{s,dyn}$	245385	[N/mm^2]	Young's modulus
$\sigma_{y,dyn}$	638.0	[N/mm^2]	dynamic yield stress
ρ	7800	[kg/m^3]	density
fibre reinforcement			
ε_{cru}	0.005	[-]	ultimate crack strain (linear soft.)

Table 1. Material properties of the beam.

3.3. Deficiencies in the computational model

There are some differences between the test and the computational model. Firstly, a full three-dimensional finite element model has not been considered because of the extreme computer costs. Furthermore, yielding or crushing of concrete in the compression zone of the beam has not been taken into account to avoid numerical problems which occur when cracking and

crushing take place in the same integration point. Finally, the shear reinforcement in the beam is left out of consideration because it does not have a large effect on the response. It is possible, though, to include it in an embedded formulation.

4. Numerical results

In this section the beam test is analysed with the abovementioned rate-independent and rate-dependent material models. Successively, the behaviour of the beam test, the question whether failure will occur in a localised or in a distributed manner and the comparison with the test, will be treated.

The structure has been analysed using a Newmark time integration scheme with a time step $\Delta t = 5 \cdot 10^{-6}$ s. The mass has been distributed in a manner that is consistent with the stiffness discretisation over the element. The nonlinear set of equations in one time step has been solved with a full Newton-Raphson method using a variation of $1 \cdot 10^{-4}$ on the reference energy norm. Especially in the stage that the crack pattern has developed completely and the steel bars slowly cause a redistribution of stresses the occurrence of many closing and re-opening cracks puts a large demand on the numerical algorithm.

Behaviour of the beam in the test

For an analysis with the coarse mesh in combination with the rate-dependent crack model the initial deformations and crack formation will be discussed. In an early stage of the test ($t = 0.001$ s; see Figure 3) we observe that the bending wave propagates from the two points of loading to the supports. At this time cracking occurs first below the two loads and propagates to the centre of the beam. When the bending wave reaches the supports the overall displacement pattern changes into a first-order vibration mode ($t = 0.002$ s; see Figure 3). In this stage the cracked zone develops and propagates in the direction of the supports. This process gradually continues until failure occurs. At $t = 0.002$ s horizontal cracking starts at the left support. It is observed that at the right support the beam tips up due to the propagation of the bending wave and reaches its maximum positive displacement at $t = 0.002$ s.

Failure in steel fibre reinforced concrete

Failure in plain concrete is accompanied by a severe localisation of deformation. By using a strain-softening continuum-based approach for the cracked material the localisation of deformation can be captured. However, for a classical rate-independent smeared crack modelling the numerical prediction of the localised cracked zone is totally unreliable (e.g. Bazant 1976). This is because the governing mathematical problem loses hyperbolicity. A possibility to prevent this loss of hyperbolicity is to include higher-order time derivative terms in the constitutive equations (Wu and Freund 1984, Needleman 1988). A rate-dependent formulation for the cracked continuum solves the mathematical problem and therefore results in reliable, mesh-insensitive computational analyses (Sluys 1992).

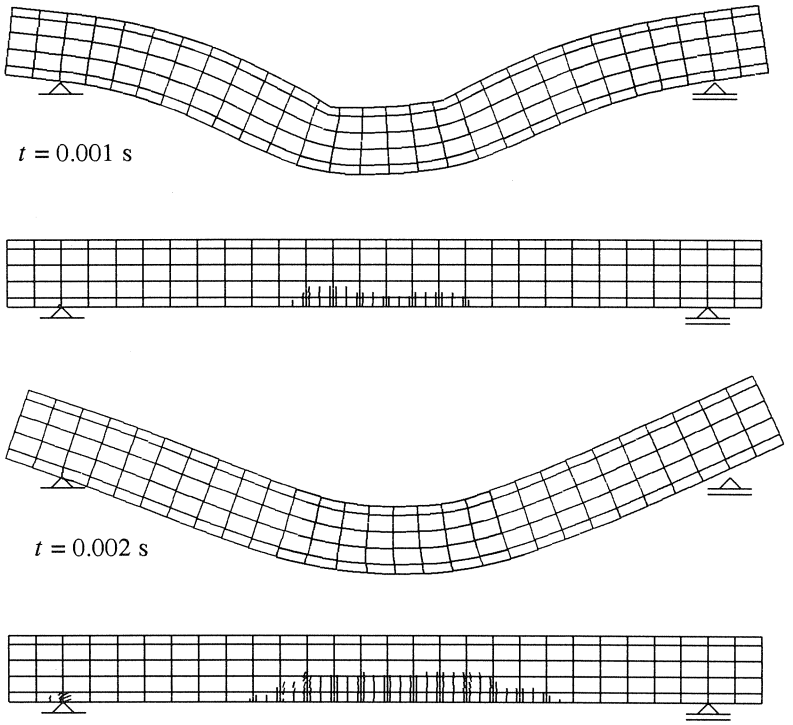

Figure 3. Crack patterns and displacements at $t = 0.001$ s and $t = 0.002$ s.

For steel fibre reinforced concrete failure occurs in a more distributed fashion. The steel reinforcement and the fibres provide the ability to the material to redistribute the stresses as soon as cracking occurs. Therefore, the crack pattern is more diffuse in comparison to localised cracking in plain concrete. Because the rate-independent crack model leads to localisation in the smallest possible zone, i.e. a line of integration points, distributed cracking can not be predicted and mesh sensitivity is present. The opposite holds for the rate-dependent model, since then distributed failure can be driven by the viscosity property of the material, which at the same time provides mesh insensitivity.

The differences between rate-independent and rate-dependent modelling of the concrete are demonstrated in the Figures 4 and 5. At a certain stage in the analysis the yield stress in the lower reinforcement bars is exceeded. Because, for the rate-independent smeared crack model, dominant crack formation occurs in one vertical row of elements plastic deformation remains restricted to one bar element. So, although the stiffness in the steel bars is slightly positive, a severe localisation of deformation occurs. In Figure 4 this is demonstrated by a qualitative picture of the beam with triangles in the integration points in which plastic deformation takes place (the size of the triangles is a measure for the plastic strain), and a

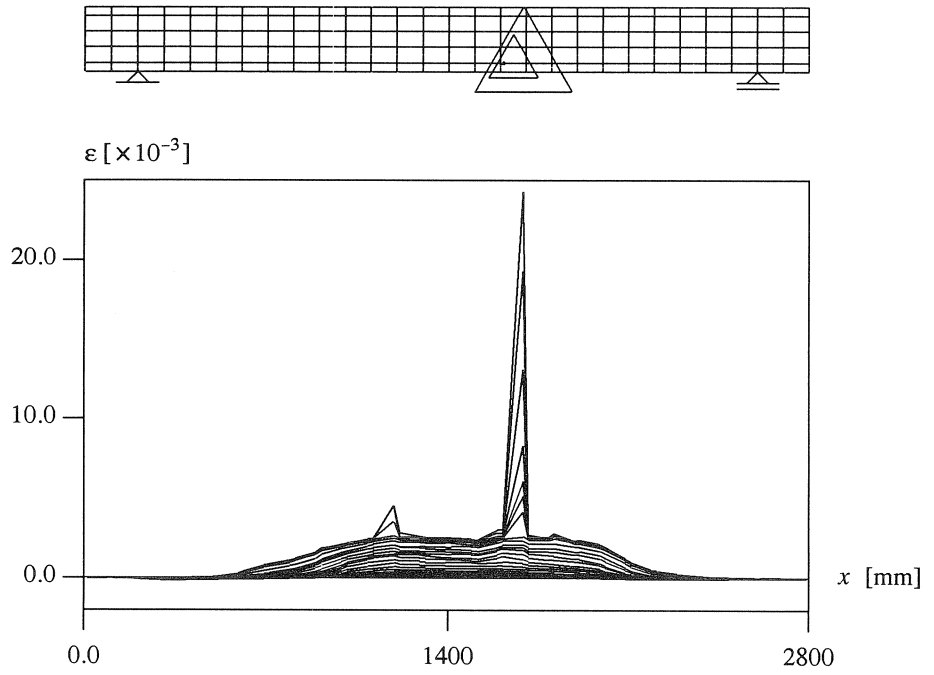

Figure 4. Plastic points (top - $t = 0.006$ s) and stroboscopic strain distributions (bottom - $0 < t < 0.006$ s) in lower steel reinforcement bar with rate-independent crack model.

quantification of the strains by a plot of the total strains along the lower reinforcement bars at several time steps.

For the rate-dependent model we observe that the zone of plastic deformation in the steel bars spreads over a number of elements. The qualitative and quantitative pictures in Figure 5 show the influence of the addition of rate-dependence. We no longer see the one-element wide localisation of deformation but a diffuse zone of plastic deformation in the steel bars. The dominant cracks appear in a zone which is equal to the zone of plastic deformation.

In fact, the real failure response of the beam is not exactly as has been determined with the rate-dependent crack model, because a zone of localised cracks occurs instead of a zone with almost uniformly distributed deformation. To model this a very fine mesh in combination with a smaller value of the viscosity is needed. Fine meshes can capture the large strain gradients which occur in the localisation process. To limit computer time the mesh should be adapted dependent on the localisation process. So-called mesh-adaptivity techniques (Ortiz and Quigley 1991, Huerta et al. 1992) should be applied to realise a fine division of elements in the cracked zone while keeping the discretisation of the rest of the beam relatively coarse.

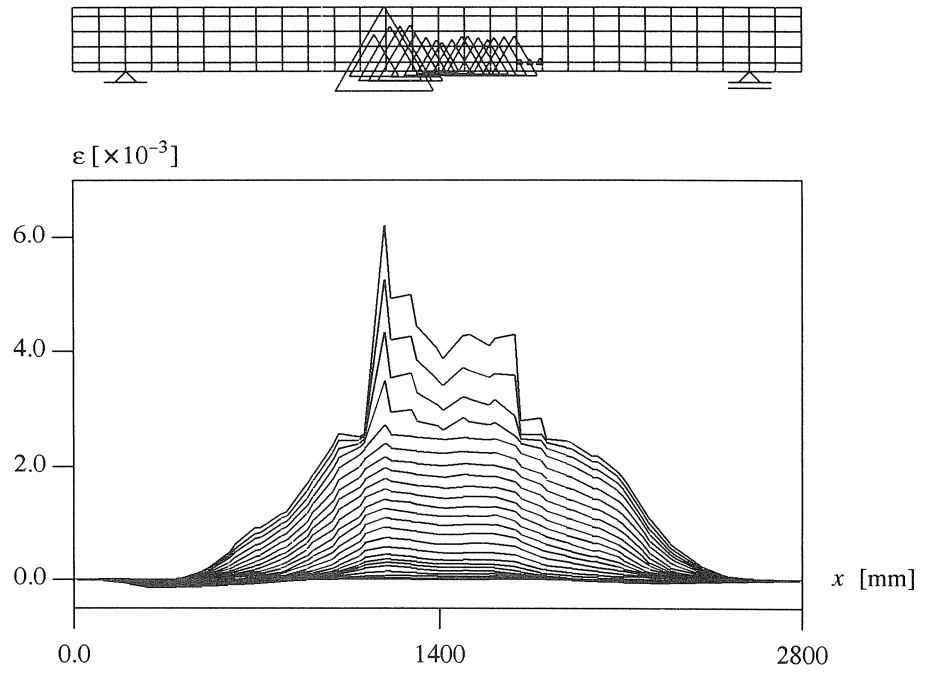

Figure 5. Plastic points (top - $t = 0.006$ s) and stroboscopic strain distributions (bottom - $0 < t < 0.006$ s) in lower steel reinforcement bar with rate-dependent crack model.

Mesh refinement

The beam has been analysed with a coarse and a fine mesh. For the analysis with the rate-independent crack model Figure 6 shows that the dominant crack for the fine mesh occurs in one vertical row of elements which does not significantly affect the overall failure mechanism. There is a slight mesh dependence because the dominating crack in the fine mesh will consume a smaller amount of energy than in the coarse mesh because the element volume belonging to the crack is smaller. However, the cracks very rapidly traverse the softening branch and full cracks occur which cause the steel bars to transmit the total force and to govern the global reponse. For this reason, in reinforced concrete analyses the shape of the strain-softening curve does not have that large influence on the global response as in plain concrete analyses. For the analyses with the rate-dependent model also the crack patterns (Figure 7) for the two meshes are equal and show the same diffuse failure pattern.

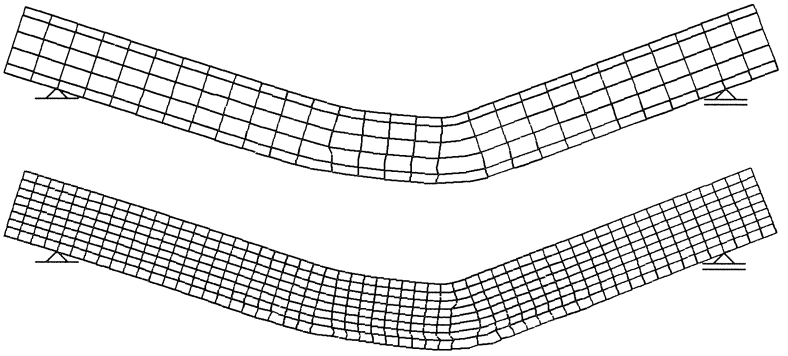

Figure 6. Deformation patterns for two different meshes with rate-independent crack model.

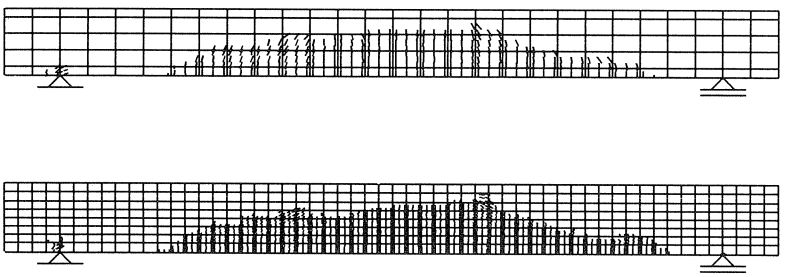

Figure 7. Crack patterns for two different meshes with rate-dependent crack model.

Comparison between computation and test

The numerical results have been compared with the test with respect to the displacement of the beam and the force in the left support (see Figure 1). The deflection-time curve for the centre of the beam has been plotted in Figure 8 for the experiment and for the rate-independent and the rate-dependent analyses (coarse mesh). For the initial stage the measured value and the numerically predicted value are in good agreement, but in a later stage a small deviation occurs. A striking result is that the difference in using a rate-independent or a rate-dependent crack model is not observable. In fact, this correspondence is logical in the light of the preceding discussion : it is mainly due to the fact that the steel bars dominate the *global* response.

The vertical force in the left support depends heavily on the stiffness k of the bilinear elastic springs. An infinite value (fixed support) resulted in a much too stiff response of the support. On the other hand, a small value for k leads to large displacements of the supports which not have been measured. In Figure 9 the numerical outcome of varying k shows the influence with respect to the test.

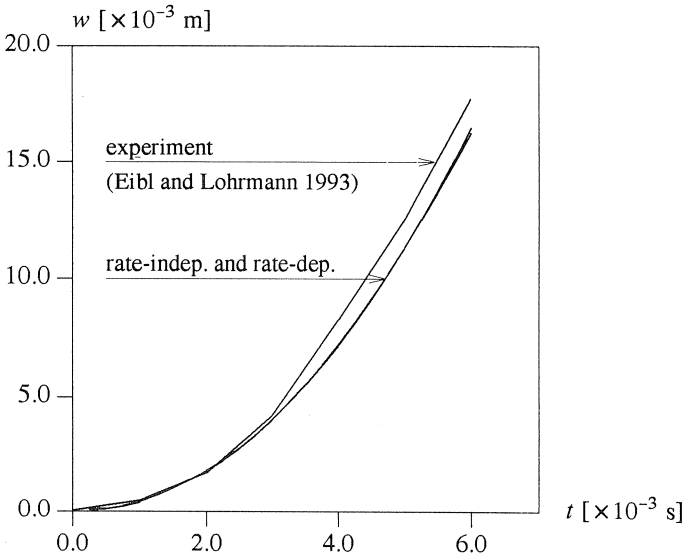

Figure 8. Deflection-time curve for centre of the beam.

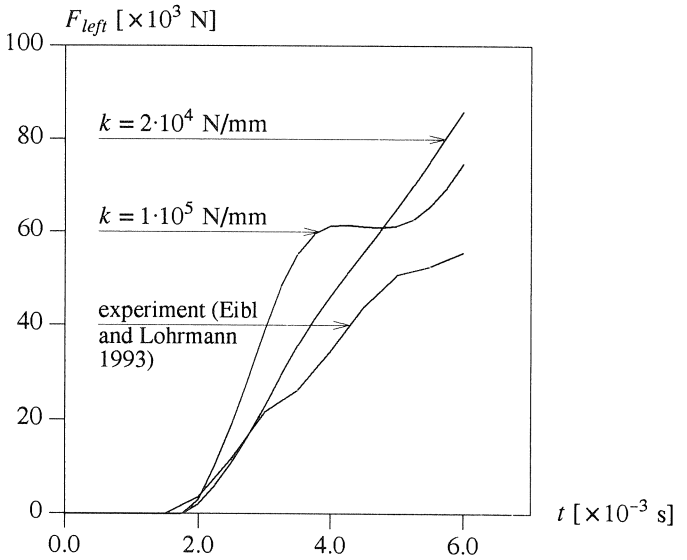

Figure 9. Force in left support against time.

5. Conclusions

The computational analysis of failure behaviour of concrete beams with conventional and steel fibre reinforcement has been carried out using rate-independent and rate-dependent smeared crack representations. In the rate-dependent formulation the distributed crack pattern is predicted correctly independent of the finite element discretisation. On the other hand, in the rate-independent case a highly localised crack distribution has been found and the strain distribution in concrete and reinforcement are dependent on the used mesh. However, the difference between a rate-independent and a rate-dependent formulation is hardly noticeable when the global response of the beam is considered.

Acknowledgements

Financial support of the Royal Netherlands Academy of Arts and Sciences to the first author and by the Commission of the European Communities through the Brite-Euram programme (project BE-3275) to the second author is gratefully acknowledged. Furthermore the authors like to direct acknowledgements to Dipl.-Ing. G. Lohrmann and to Prof.Dr.-Ing. J. Eibl of the Institut für Massivbau und Baustofftechnologie from Karlsruhe University for providing the experimental data.

References

BAZANT, Z.P. (1976) - Instability, ductility and size effect in strain softening concrete, *ASCE J. Eng. Mech.*, **102(2)** , pp. 331-344.

BORST, R. de and NAUTA, P. (1985) - Non-orthogonal cracks in a smeared finite element model, *Eng. Comp.*, **2(1)** , pp. 35-46.

DORR, K. (1980) - *Ein Beitrag zur Berechnung von Stahlbetonscheiben unter besonderer Berücksichtiging des Verbundverhaltens*, Dissertation, University of Darmstadt, Darmstadt.

EIBL, J. and LOHRMANN, G. (1993) - *Verification experiments on FRC structural elements: Dynamic loading*, BRITE/EURAM Project BE-89-3275, Report on Subtask 5.3, University of Karlsruhe, Karlsruhe (in preparation).

HUERTA, A., PIJAUDIER-CABOT, G. and BODE, L. (1992) - 'ALE formulation in nonlocal strain softening solids', *Proc. Conf. on Computational Plasticity, Fundamentals and Applications, Part II*, Eds. D.R.J. Owen, E. Oñate and E. Hinton, Pineridge Press, Swansea, pp. 2249-2268.

KORMELING, H.A. (1986) - *Strain rate and temperature behaviour of steel fibre concrete in tension*, Dissertation, Delft University of Technology, Delft.

NEEDLEMAN, A. (1988) - Material rate dependence and mesh sensitivity on localisation problems, *Comp. Meth. Appl. Mech. Eng.*, **67** , pp. 69-86.

ORTIZ, M. and QUIGLEY, J.J. (1991) - Adaptive mesh refinement in strain localization problems, *Comp. Meth. Appl. Mech. Eng.*, **90** , pp. 781-804.

ROTS, J.G. (1988) - *Computational modeling of concrete fracture*, Dissertation, Delft University of Technology, Delft.

SLUYS, L.J. (1992) - *Wave propagation, localisation and dispersion in softening solids* Dissertation, Delft University of Technology, Delft.

WU, F.H. and FREUND, L.B. (1984) - Deformation trapping due to thermoplastic instability in one-dimensional wave propagation, *J. Mech. Phys. Solids*, **32(2)** , pp. 119-132.

ZIELINSKI, A.J. (1982) - *Fracture of concrete and mortar under uniaxial impact tensile loading*, Dissertation, Delft University of Technology, Delft.